Ionic Liquid Electrolytes for Lithium–Sulfur Batteries

ARTICLE *in* THE JOURNAL OF PHYSICAL CHEMISTRY C · SEPTEMBER 2013

Impact Factor: 4.77 · DOI: 10.1021/jp408037e

THE JOURNAL OF PHYSICAL CHEMISTRY C

Article

pubs.acs.org/JPCC

Ionic Liquid Electrolytes for Lithium−Sulfur Batteries

Jun-Woo Park, Kazuhide Ueno, Naoki Tachikawa, Kaoru Dokko, and Masayoshi Watanabe*

Department of Chemistry and Biotechnology, Yokohama National University, 79-5 Tokiwadai, Hodogaya-ku, Yokohama 240-8501, Japan

Supporting Information

ABSTRACT: A variety of binary mixtures of aprotic ionic liquids (ILs) and lithium salts were thoroughly studied as electrolytes for rechargeable lithium−sulfur (Li−S) batteries. The saturation solubility of sulfur and lithium polysulfides (Li_2S_m), the active materials in the Li−S battery, in the electrolytes was quantitatively determined, and the performance of the Li−S battery using the electrolytes was also investigated. Although the solubility of nonionic sulfur was low in all of the electrolytes evaluated, the solubility of Li_2S_m in the IL-based electrolyte was strongly dependent on the anionic structure, and the difference in the solubility could be rationalized in terms of the donor ability of the IL solvent. Dissolution of Li_2S_m in the ILs with strong donor ability was comparable to that achieved with typical organic electrolytes; the strongly donating IL electrolyte did not prevent redox shuttle reaction in the Li−S cells. The battery performance was also influenced by unfavorable side reactions of the anions (such as tetrafluoroborate (BF_4^-) and bis(fluorosulfonylamide) ($[FSA]^-$)) with polysulfides and by slow mass transport in viscous ILs, even though the dissolution of Li_2S_m into the IL electrolyte was greatly suppressed. Among the IL-based electrolytes, the low-viscosity [TFSA]-based ILs facilitated stable charge/discharge of the Li−S batteries with high capacity and high Coulombic efficiency. The unique *solvent effect* of the ILs can thus be exploited in the Li−S battery by judicious selection of ILs that exhibit high lithium-ion-transport ability and electrochemical stability in the presence of Li_2S_m.

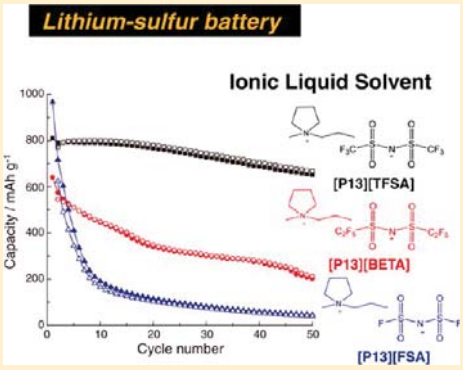

1. INTRODUCTION

Room-temperature ionic liquids (ILs) are liquids at room temperature and composed of entirely of ions. A number of studies on ILs as alternatives to volatile molecular solvents have been carried out,[1] given that typical ILs exhibit many attractive properties, including negligibly low volatility, low flammability, high thermal stability, and a wide liquidus range. Other favorable properties such as high ionic conductivity and the wide electrochemical potential window have further encouraged the use of ILs as electrolytes for lithium secondary batteries for improved battery safety. Thus, binary mixtures of an aprotic IL and a Li salt have been studied as safer lithium-conducting electrolytes for lithium secondary batteries using a variety of anode and cathode materials.[2,3]

Elemental sulfur (S_8) is a low cost and abundantly available cathode material with a theoretical capacity of 1672 mA·hg^{-1}, which is 10-fold higher than that of transition-metal oxide cathodes utilized in Li-ion batteries, thus fueling the burgeoning interest in rechargeable lithium−sulfur (Li−S) batteries as promising candidates for next-generation high-energy storage devices.[4−6] However, the practical application of Li−S cells is limited by two major limitations: (i) the insulating nature and sluggish electrochemical reactions of the sulfur cathode and (ii) dissolution of the reaction intermediates, lithium polysulfides (Li_2S_m), into the electrolyte. The poor electrical conductivity and low utilization of sulfur have recently been addressed by fabricating composite sulfur cathodes with nanostructured carbon materials,[7−10] nanocarbons,[11−13] and conducting polymers[11,14] to circumvent the former; in contrast, the dissolution of the reaction intermediates in the electrolyte still needs to be improved in order to achieve a long life for Li−S batteries with high energy density.

The dissolution of Li_2S_m results in unfavorable side reactions as well as loss of the active material from the cathode. It is well-known that carbonate-based solvents such as ethylene carbonate (EC) and diethyl carbonate (DEC) react irreversibly with polysulfides; thus, solvents stable against nucleophilic attack of polysulfides must be selected.[15] Even if an electrolyte solution is chemically stable in the presence of polysulfides, the solubilized Li_2S_m species may still be reduced at the Li metal anode, and the resulting lower order intermediates are then oxidized at the cathode during cell charging. This series of events is known as the redox shuttle mechanism; it leads to low Coulombic efficiency and rapid capacity fading.[16−18]

Many strategies have been attempted to inhibit the side reactions caused by the dissolution of Li_2S_m into the electrolyte by focusing on the various components of Li−S batteries. The most widely utilized strategy involves the formation of a passivation layer on the Li metal anode using ether-based mixture electrolytes containing $LiNO_3$ as an additive.[19,20] Lin et

Received: August 11, 2013
Revised: September 14, 2013
Published: September 16, 2013

al. recently reported that P_2S_5 is also an effective additive for the passivation of the lithium metal surface.[21] The redox shuttle process is prevented by the protective film, whereas the ether-based electrolytes containing excess solvents readily dissolve higher-order Li_2S_m species ($m > 2$), and behave as a *catholyte* after the first discharge in the Li−S cells.[20] Modification of sulfur cathodes with polymer coatings[7,11] and addition of a mesoporous silica as a polysulfide reservoir in the composite cathode have also been attempted to limit the dissolution of Li_2S_m.[22] Both polymer[23] and inorganic solid electrolytes[24,25] offer a physical (or kinetic) barrier to Li_2S_m dissolution, and thus, have been evaluated as electrolytes for the Li−S battery.

Among the various strategies attempted,[26] the design of *liquid* electrolytes with potentially lower solubilizing power for Li_2S_m may be the most straightforward and the most valid approach for suppressing polysulfide dissolution. A liquid electrolyte targeted toward this purpose should act as a poor solvent for all of the redox-active species of the sulfur cathode, such as S_8 and Li_2S_m, while ensuring high Li^+ conduction by the originally doped Li salts. This requirement is somewhat rigorous given that the active spices exhibit a wide range of hydrophilic−hydrophobic character: the most hydrophobic S_8 is only soluble in nonpolar solvents such as benzene, whereas the final reduction product, Li_2S, is only soluble in highly polar solvents such as water. Polysulfides are expected to exhibit intermediate character between the pure species, depending on the chain length of Li_2S_m. In short, a solvent that does not dissolve any of the active species (S_8 and Li_2S_m) but sufficiently dissolves the Li salt is required for the *liquid* electrolyte. A certain ionic liquid electrolyte was found to meet these stringent requirements;[27−30] in previous work, we demonstrated that the Li-salt-doped IL, *N*,*N*-diethyl-*N*-methyl-*N*-(2-methoxyethyl)ammonium bis(trifluoromethanesulfonyl)amide ([DEME][TFSA]), was an excellent electrolyte for the Li−S battery, where dissolution of the active materials was strongly suppressed because of the unique *solvent effect* of the IL, compared to ether-based organic electrolytes.[29] However, the dependence of the solubility of S_8 and Li_2S_m and the resulting Li−S battery performance on the ionic structure of the ILs is not yet understood, even though a variety of cation−anion combinations (termed "designer solvents") are available for tuning the properties of ILs.[31]

Herein, we report the performance of a Li−S battery using binary mixtures of lithium salts (LiX) and aprotic ILs. The saturation solubility of the active materials in the IL-based electrolytes is quantitatively determined, and the effects of the ionic structure on the capacity and the cycle ability of the Li−S cells are investigated. Although the IL-based electrolyte has been demonstrated to be promising as a Li−S battery electrolyte,[27,29] the battery performance was found to be strongly dependent on the ionic structure of the IL solvent. The importance of the IL solvent for the successful operation of the Li−S battery is discussed in light of the solubility of Li_2S_m, transport property of the electrolyte, and electrochemical stability of the ILs themselves in the Li−S battery.

2. EXPERIMENTAL SECTION

Materials. The ionic liquids used in this study comprise a pair of the following organic cations and fluorinated anions: *N*,*N*-diethyl-*N*-methyl-*N*-(2-methoxyethyl) ammonium ($[DEME]^+$), *N*-methyl-*N*-propylpyrrolidinium ($[P13]^+$), *N*-butyl-*N*-methylpyrrolidinium ($[P14]^+$), 1-butyl-2,3-dimethylimidazolium ($[C_4dmim]$), *N*-methyl-*N*-propyl piperidinium ($[PP13]^+$), and triethylpentylphosphonium ($[P2225]^+$) as cations; and bis(trifluoromethanesulfonyl)amide ($[TFSA]^-$), bis(fluorosulfonyl)amide ($[FSA]^-$), bis-(pentafluoroethanesulfonyl)amide ($[BETA]^-$), trifluoromethanesulfonate ($[OTf]^-$), and tetrafluoroborate ($[BF_4]^-$) as anions. $[C_4dmim][TFSA]$ and [P14][OTf] were obtained from IoLiTec and used as received. [P13][BETA] was prepared by the metathesis reaction of [P13]Br with Li[BETA], and purified according to the standard method used for hydrophobic ILs.[32] The other ILs were purchased from Kanto Kagaku and used as received, unless otherwise noted. The water content of each IL was checked via Karl Fischer titration using a Mitsubishi Chemical CA-07 moisture meter. All of the values were lower than 50 ppm, except for the values of 230 and 280 ppm obtained for $[C_4dmim][TFSA]$ and [P14][OTf], respectively. $LiPF_6$, $LiBF_4$, and Li[BETA] were purchased from Kishida Chemical (battery grade) and used as received. Li[TFSA] was obtained from Morita Chemical and was dried under high vacuum at 120 °C for 12 h prior to use.

The sulfur composite cathode was prepared in a manner similar to that of a previously reported method.[29,30] Elemental sulfur (S_8, 99.99%, Wako) and Ketjen black (KB, EC600JD, Lion Corporation) were mixed in a weight ratio of 2:1 and heated to 155 °C for 8 h to form the S_8/KB composite. The composite was then mixed with polyvinyl alcohol (PVA, partially hydrolyzed, average degree of polymerization: 3100−3900, Wako) dissolved in *N*-methyl-2-pyrrolidinone. After homogenization, the slurry was coated onto a 20-μm-thick aluminum current collector and dried at 80 °C for 12 h. The composition of the composite electrode is 60 wt % for S_8, 30 wt % for KB, and 10 wt % for PVA. The prepared composite sheet was cut into a circular shape (16 mm diameter) and compressed at 100 kgf·cm^{-2}. The thickness of the composite electrode was ca. 17 μm, and the mass of S_8 on the sheet electrode was ca. 1.2 mg.

Measurements. The saturation solubility of S_8 and Li_2S_m in the IL electrolytes was evaluated according to the reported procedure.[29,30] The saturated solutions of Li_2S_m were prepared from the stoichiometric mixtures of S_8 and Li_2S (Aldrich) at molar ratios of 7:8, 3:8, and 1:8, which correspond to the nominal chemical structures Li_2S_8, Li_2S_4, and Li_2S_2, respectively. The solutions were heated and stirred at 60 °C for 5 days and allowed to stand for 2 days at room temperature. The solid residue was separated using a centrifuge, and the supernatant solution was diluted with 1 mol·dm^{-3} Li[TFSA] in the tetraglyme (TEGDME) solution to achieve a suitable concentration. The diluted Li_2S_m solutions were then electrochemically oxidized to S_8 using a potential step of 3 V, in a two-compartment cell having a porous glass filter as a separator, and a carbon felt as a working electrode, and lithium metal foil as a counter electrode. The maximum absorption of S_8 oxidized from the polysulfides was recorded using a UV−vis spectrometer (UV-2500PC, Shimadzu). The donor ability of the ILs was evaluated based on the maximum UV−vis absorption wavelength (λ_{Cu}) of a copper complex solvatochromic indicator, (acetylacetonate) (*N*,*N*,*N*′,*N*′-tetramethylethylenediamine) copper(II) tetraphenylborate ([Cu(acac)(tmen)][BPh_4]),[33] dissolved in ILs in the same way as reported in our previous work.[34]

The ionic conductivity was measured in the frequency range 500 kHz−1 Hz by the complex impedance method using 10 mV amplitude (VMP2, Princeton Applied Research). Two platinum black electrodes (CG-511B, TOA Electronics, cell

dx.doi.org/10.1021/jp408037e | J. Phys. Chem. C 2013, 117, 20531−20541

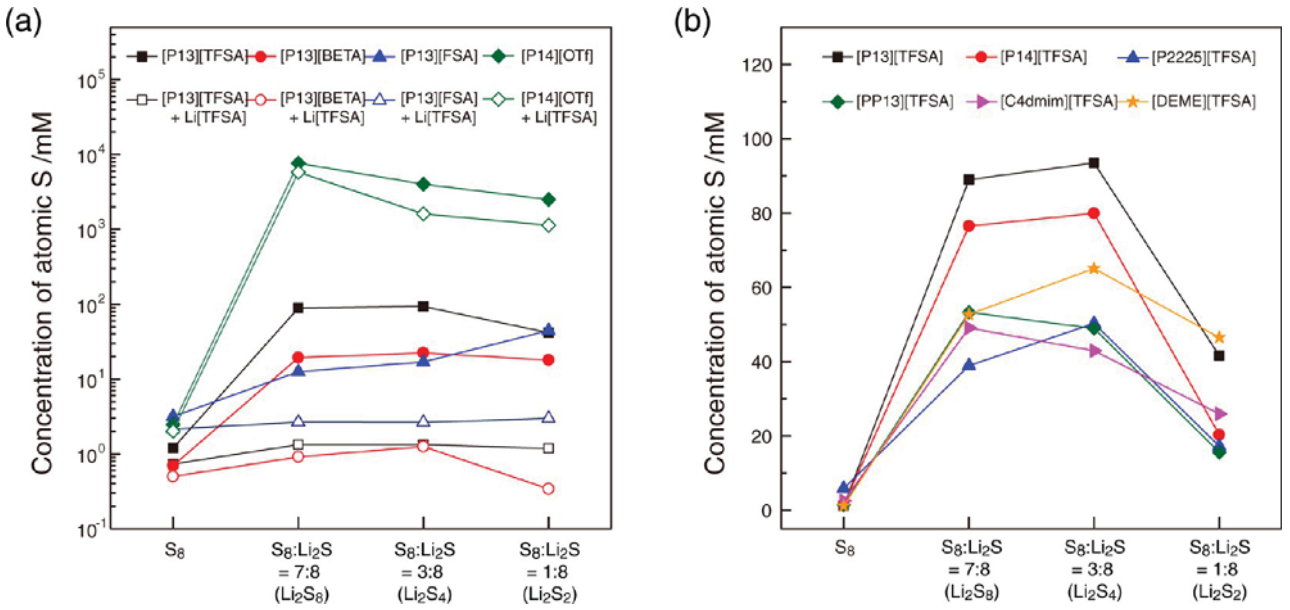

Figure 1. Saturation concentrations of S_8 and mixtures of S_8 and LiS_2 (Li_2S_m), represented in units of total atomic−S concentration (a) in pyrrolidinium ILs with different anions in the absence and presence of 0.5 mol·kg^{-1} Li[TFSA] (on semilogarithmic scale), and (b) in [TFSA]-based ILs with different cations without Li[TFSA].

constant = ca. 1 cm^{-1}) were dipped in the electrolyte, and the sample cell was thermally equilibrated at each temperature for at least 90 min using a thermostat chamber. The temperature dependences of the viscosity and density were measured using SVM3000 (Anton Paar). Pulsed-gradient spin−echo nuclear magnetic resonance (PGSE-NMR) measurements were performed using a JEOL ECX400 spectrometer with a 9.4 T narrow bore superconducting magnet equipped with a JEOL pulse field gradient probe to determine the self-diffusion coefficients of lithium cations (^{7}Li, 155.3 MHz) in the IL electrolyte.[35,36] The decomposition of the electrolytes in the presence of Li_2S_m was monitored using multinuclear NMR measurements performed using the aforementioned spectrometer. A sample tube with a double tube structure (SC-212 008, Shigemi) was used for the measurements.

The 2032-type coin cell with a KB/S_8 composite cathode (electrode area: ∼2 cm^2, weight of sulfur on the composite electrode: ∼1.2 mg), porous glass separator (GA-55, Advantec), Li metal anode, and an IL-based electrolyte was assembled in an Ar-filled glovebox. Galvanostatic charge/discharge measurements (HJ1001SD8, Hokuto Denko) were performed with cutoff potentials of 1.5 and 3.3 V at 30 °C in a thermostatted chamber. Because the Li−S cell is prepared in the fully charged state, the charge/discharge cycle was defined as follows: first discharge → second charge → second discharge → third charge → third discharge, and so forth. The Coulombic efficiency was defined as: (*N*th discharge capacity)/(*N*th charge capacity). The specific capacity of the cell was calculated based on the mass of S_8.

After the charge/discharge cycles, the coin cell was disassembled in the charged state in the glovebox, and the composite cathode was thoroughly washed with a large amount of dimethoxyethane followed by drying under vacuum. The surface morphology of the composite cathode was evaluated using scanning electron microscopy (S-2600N, Hitachi). The X-ray diffraction (XRD) patterns of the composite cathodes were collected in the 2θ range 10−90° on RINT-2000 (Rigaku) using Cu Kα radiation.

3. RESULTS AND DISCUSSION

Solubility of S_8 and Li_2S_m in ILs. In a previous work,[29] we demonstrated that the solubility limit of Li_2S_m, especially of higher order polysulfides (m > 4), in 0.64 M Li[TFSA] in [DEME][TFSA] was significantly lower than that in a typical organic electrolyte, 0.98 M Li[TFSA] in TEGDME. Successful control of the polysulfide dissolution gave rise to highly reversible charge/discharge in the Li−S cell with high Coulombic efficiency, exceeding 98%.

The very low solubility of Li_2S_m in the IL-based electrolyte can be explained in terms of the donor ability of the electrolyte solutions. Dissolution of ionic Li_2S_m is thought to be principally dominated by the solvation of the Li^+ ions of polysulfides with the electrolyte molecules. Because of the weak Lewis basicity of the charge-delocalized [TFSA] anion, the Gutmann donor number (DN) for [DEME][TFSA] was ca. 10 kcal·mol^{-1},[29] indicating that its donor ability is lower than that of organic solvents (*cf.* DN = 16.6 kcal·mol^{-1} for TEGDME[37]). Although [TFSA] anions are able to solvate the Li^+ ions of Li_2S_m, some portions of [TFSA] anions in the electrolyte already interact with Li^+ of originally doped Li[TFSA] in the form of $Li[TFSA]_2$,[38] further attenuating the donor ability of the Li-doped IL electrolyte. Herein, we verify this postulate for the suppression of Li_2S_m dissolution using other ILs with different ionic structures.

The saturation solubility of S_8 and Li_2S_m in the ILs is shown in Figure 1. Polysulfide solutions with three different ratios of S_8 and Li_2S—Li_2S_8, Li_2S_4, and Li_2S_2—were studied in this work. However, note that the nominal Li_2S_m composition was not achieved; rather, a "mixture" of polysulfides with different chain lengths was obtained because of the disproportional reaction.[39] Therefore, the saturated "mixture" of the polysulfides was first electrochemically oxidized to pure S_8, and then the amount of converted S_8 was quantified as the saturated concentration of Li_2S_m. The solubility limit in the solution was given as total atomic−S concentration.

Although the actual composition of the mixture of Li_2S_m could not be determined, the results presented in Figure 1

dx.doi.org/10.1021/jp408037e | J. Phys. Chem. C 2013, 117, 20531−20541

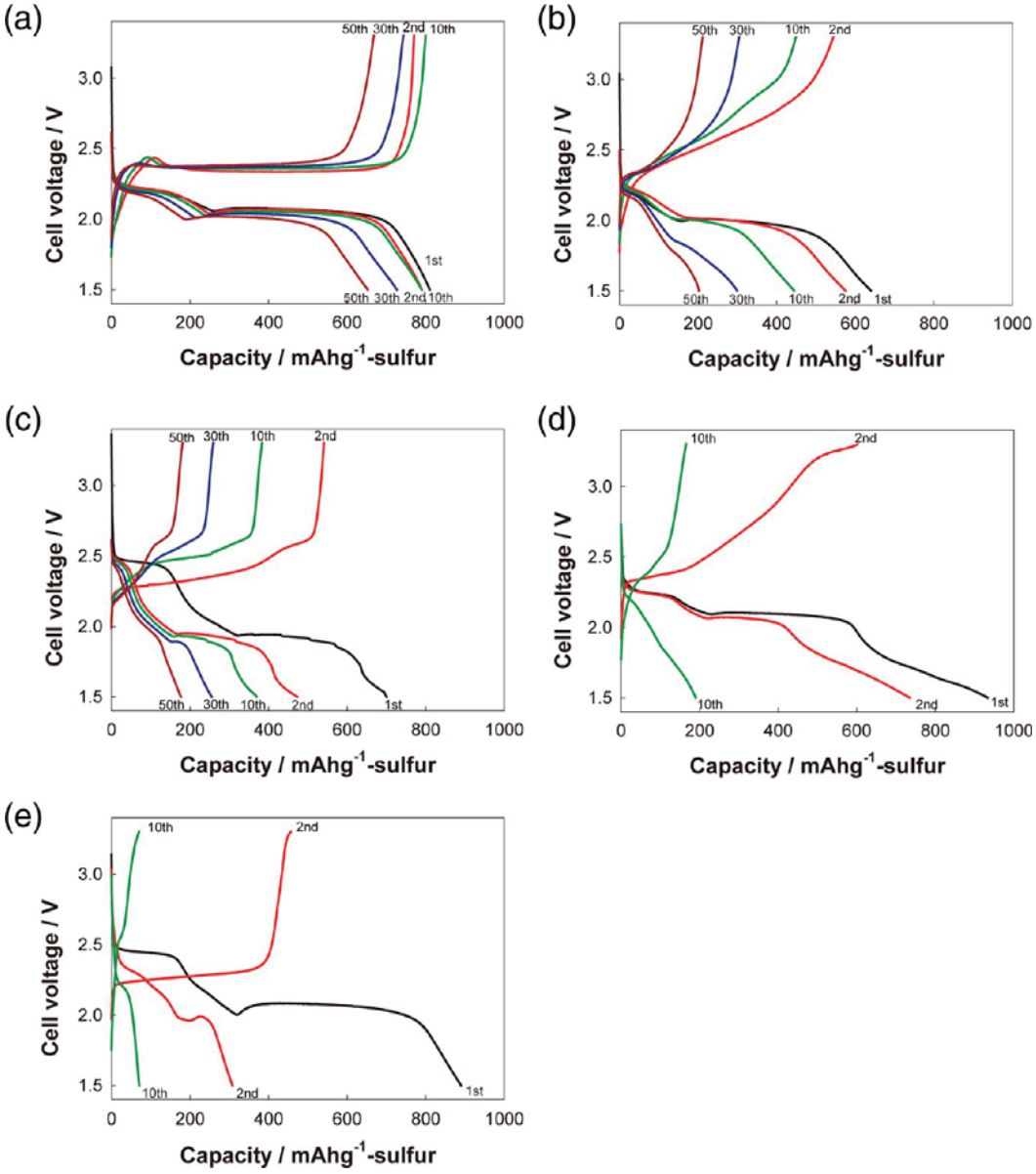

Figure 2. Galvanostatic charge/discharge curves of Li–S cells using ILs containing 0.5 mol·kg^{-1} of Li[TFSA] at constant current density of 139 mA·g^{-1}-sulfur, at 30 °C: (a) [P13][TFSA], (b) [P13][BETA], (c) [P14][OTf], (d) [P13][FSA], (e) [DEME]BF_4.

suggest that longer Li_2S_m ($m > 4$) are more likely to be soluble in most of the ILs. Figure 1a shows the solubility limit of S_8 and Li_2S_m in pyrrolidinium-based ILs with different anionic structures in the absence and presence of 0.5 mol·kg^{-1} of Li[TFSA]. The difference in the saturation concentration of nonionic S_8 in various ILs is marginal, even in the presence of Li[TFSA], and all the values were lower than 4 mM. In contrast, the solubility of Li_2S_m was strongly dependent on the anionic component of the ILs. It is striking that the solubility of Li_2S_m in [P14][OTf] exceeds 2500 mM for all compositions of Li_2S_m, which is nearly 2 orders of magnitude higher than the solubility in the other ILs—[P13][TFSA], [P13][FSA], and [P13][BETA]. Moreover, the solubility of the polysulfides in [P14][OTf] (7660 mM for Li_2S_8) is even higher than that in the organic electrolyte, TEGDME (6050 mM for Li_2S_8).[29]

When 0.5 mol·kg^{-1} of Li[TFSA] is added to the ILs, the solubility of Li_2S_m decreased to the same level as that of nonionic S_8. These results are consistent with our previous findings for [DEME][TFSA].[29] We also confirmed a similar suppression of polysulfide dissolution in [DEME][TFSA] with different Li salts such as $LiPF_6$ and Li[BETA] (see Supporting Information Figure S1a). However, [P14][OTf] is the obvious exception: the solubility of Li_2S_m was only slightly lowered, even with the addition of Li[TFSA]. Although BF_4^-, another common anion, was also evaluated, the polysulfide solubility in BF_4^--based IL electrolytes such as [DEME]BF_4 and a binary mixture of [DEME][TFSA] and $LiBF_4$ was not successfully determined. The oxidation reaction of the polysulfides did not occur because of an irreversible chemical reaction of the BF_4 anion with polysulfides. A detailed discussion is presented in a later section.

To examine the relationship between the solubility of Li_2S_m and the donor ability of IL solvents, the λ_{Cu} value of a solvatochromic probe, [Cu(acac)(tmen)][BPh_4], in the ILs was determined, where λ_{Cu} gives a good correlation with Gutmann DN.[33] In the case of ILs, λ_{Cu} is predominantly determined by

dx.doi.org/10.1021/jp408037e | J. Phys. Chem. C 2013, 117, 20531–20541

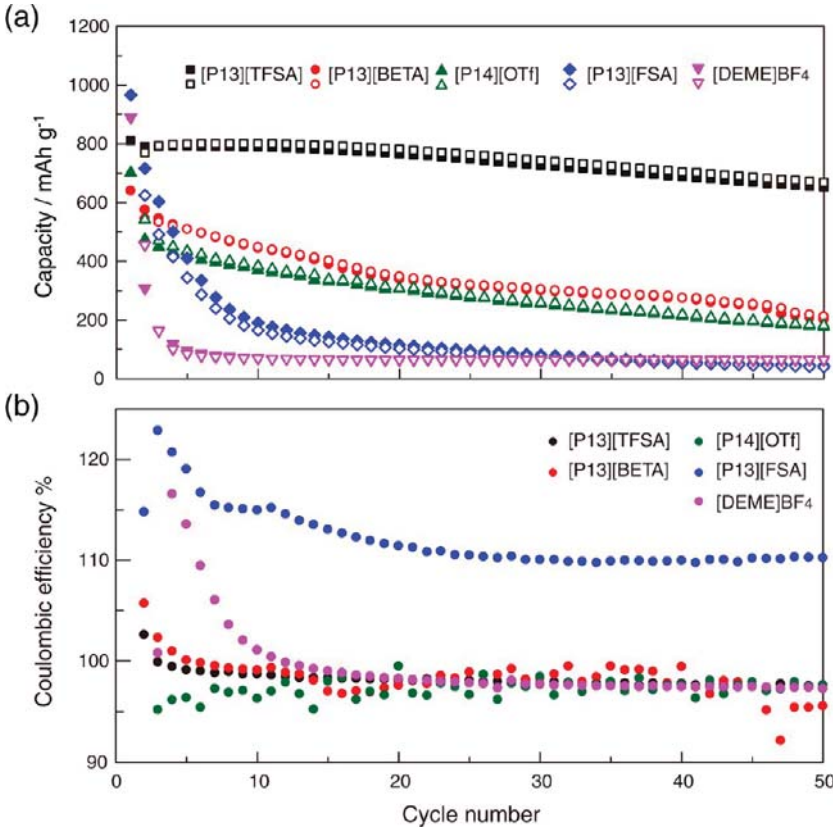

Figure 3. Cycling performance of Li−S cells using IL electrolytes with different anions, at a constant current density of 139 m·Ag^{1-}-sulfur, for (a) capacity and (b) Coulombic efficiency. Open and closed plots in (a) represent charge and discharge capacities, respectively.

Table 1. Viscosity (η), Ionic Conductivity (σ), and Lithium Molar Concentration (c) for IL Electrolytes Containing 0.5 mol·kg^{-1} of Li[TFSA], at 30 °C

ionic liquid	η (mPa s)	σ (mS cm^{-1})	D_{Li} (10^{-7} cm^2 s^{-1})	c (mol dm^{-3})
[P13][TFSA]	136	2.0	0.57	0.64
[P13][BETA]	507	0.47	0.16	0.68
[P13][FSA]	52.3	6.4	1.9	0.61
[P14][OTf]	278	1.1	0.20	0.57
[DEME][BF_4]	357	1.2	0.26	0.54
[P14][TFSA]	167	1.4	0.42	0.63
[P2225][TFSA]	162	0.92	0.47	0.59
[PP13][TFSA]	324	0.78	0.21	0.64
[C_4dmim][TFSA]	167	1.4	0.41	0.64
[DEME][TFSA]	137	1.4	0.63	0.64

the anionic structure.[34] The measured λ_{Cu} was almost the same (544−546 nm) for [P13][TFSA], [P13][FSA], and [P13][BETA]. In contrast, [P14][OTf] gave a higher value of λ_{Cu} ~581 nm, indicating its stronger donor property. Actual DNs of 11.2, 7.2, and 20.4 kcal·mol^{-1} were reported for [C_2mim][TFSA], [C_2mim][BETA], and [C_2mim][OTf], respectively, by van Eldik et al.[40] If the anionic structure was similar, the DNs for the pyrrolidinium ILs used in the present study should be comparable to the reported DNs for the [C_2mim]-based ILs. Therefore, the significantly high solubility of Li_2S_m in [P14][OTf] can be attributed to the strong donor ability of the solvent. Indeed, the DN of [P14][OTf] would be even higher than that of TEGDME, consistent with the higher solubility of Li_2S_m in [P14][OTf] than in the organic TEGDME electrolyte. These results suggest that the competition between the anion of the ILs and the polysulfides to interact with Li^+ ions dominates the dissolution of Li_2S_m. The solvation of Li^+ ions by the anions stronger than (or comparable to) S_m^{2-} (e.g., $[OTf]^-$) results in dissociation of Li_2S_m and high solubility of S_m^{2-}. In the ILs with the anions weaker than S_m^{2-} (e.g., $[TFSA]^-$ and PF_6^-),[34] on the other hand, Li^+ ions prefer to exist in form of Li_2S_m because of poor solvation property of the weak anions. Note that the donor ability (or Lewis basicity) of S_m^{2-} changes depending on the chain length (m). Indeed, the S_m^{2-} with $m \geq 4$, which is expected to have relatively weak donor ability (Lewis basicity) due to the large ionic size, shows relatively high solubility in the ILs (Figure 1). In contrast, the solubility of S_2^{2-} with small ionic size and high Lewis basicity is lower than that of larger S_m^{2-} ($m \geq 4$). Consequently, the donor ability theory can explain the polysulfide solubility even in the IL media. Importantly, these results also emphasize that not all ILs are effective for suppressing the polysulfide dissolution in Li−S cells.

Minor differences in the solubility of Li_2S_m are observed by comparing the ILs with fluorinated sulfonylamide anions (Figure 1a) and [TFSA]-based ILs with different cations (Figure 1b). For the ILs with [TFSA] derivatives, the solubility of Li_2S_m (m = 8 and 4), based on the anion, increased in the order: $[TFSA]^- > [BETA]^- > [FSA]^-$. The lower solubility of these species in [P13][BETA] than in [P13][TFSA] could be ascribed to the weaker donor ability (DN) of [P13][BETA]; however, their low solubility in [P13][FSA] may be associated with a different Li^+ solvation structure in this IL. Li^+ was solvated in the form of $[Li(FSA)_3]$,[41,42] which differs from the

dx.doi.org/10.1021/jp408037e | J. Phys. Chem. C 2013, 117, 20531−20541

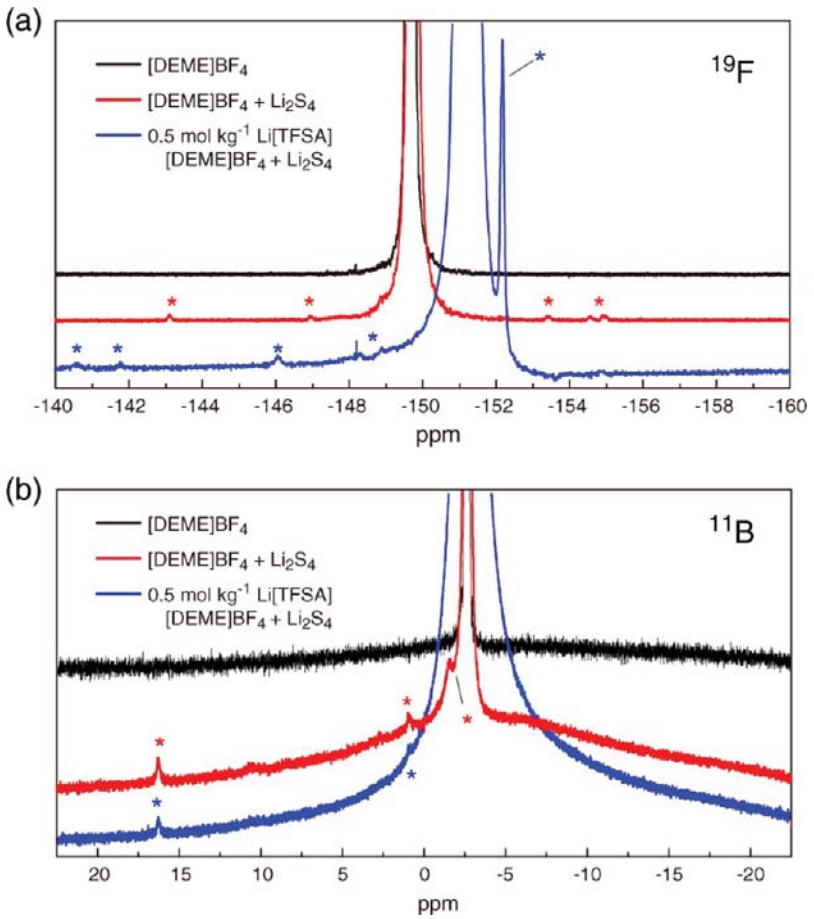

Figure 4. NMR spectra of $[DEME]BF_4$ before (black) and after (red and blue) mixing with Li_2S_4, (a) ^{19}F-NMR, and (b) ^{11}B-NMR. Saturated solutions of Li_2S_4 in electrolytes were used for measurement. Asterisks represent peaks from byproducts.

well-known $[Li(TFSA)_2]$ complex in [TFSA]-based ILs.[38] Thus, the increased number of anions required for Li^+ solvation may result in the lower solubility limit in [P13][FSA]. The solubility of Li_2S_m with different cations (Figure 1b) increased in the order: $[P13]^+ > [P14]^+ > [DEME]^+ > [PP13]^+ > [C_4dmim]^+ > [P2225]^+$ for Li_2S_8. The solubility of Li_2S_m was apparently lower for the [TFSA]-based ILs with larger cations.[43] A similar explanation may also be drawn for the anionic size of ILs besides the DN effect: the pyrrolidinium-based ILs with bulky sulfonylamide anions exhibited much lower solvency for Li_2S_m compared with [P14][OTf]. According to Welton et al.,[44] the dissolution of ionic solutes in molecular solvent-free ILs takes place thorough the metathesis reaction of the ionic solute and solvent. If the size of the ionic solutes and ions of ILs matched, site exchange may occur readily. Therefore, the solubility appears to also be influenced by similarity (or dissimilarity) of the ionic size of S_m^{2-} or the ion clusters of the polysulfides (e.g., LiS_m^- and $Li_3S_m^+$) and IL solvents, in addition to the polarity scales such as DN.

Battery Performance Using IL Electrolytes. Figure 2 shows the galvanostatic charge/discharge tests using the ILs with different anions at a slow charge/discharge current rate of 139 $mA{\cdot}g^{-1}$-sulfur (1/12 C rate) at 30 °C. The summarized cycle performance is shown in Figure 3. It was found that the anionic structure of the IL electrolytes had a major impact on the battery performance. Reversible charge/discharge of the Li−S cell was achieved only with the [P13][TFSA] electrolyte (Figures 2 and 3), whereas each of the other electrolytes had an adverse effect on the stable charge/discharge of the Li−S cell. The poor battery performance with these electrolytes did not originate only from the dissolution of Li_2S_m, but also from other factors such as unfavorable side reactions and slower mass transport through the electrolyte.

The Li−S cell employing [P13][TFSA] (Figure 2a) shows two voltage plateaus of approximately 2.3 and 2.0 V in the discharge curves, whereas only one plateau region, at ca. 2.4 V, is apparent in the charge curves. These voltage plateaus do not change significantly during repeated charge/discharge cycles after 50 cycles, although the capacity decreased gradually with the cycle number. The two voltage regions in the discharge curves are considered as the reduction voltages of S_8 to longer order Li_2S_m ($m \geq 4$) for the higher voltage, and the reduction of Li_2S_m to Li_2S for the lower voltage, respectively.[30] These voltage plateaus in the charge/discharge curves are consistent with previous results of the Li−S cell obtained by employing [DEME][TFSA].[29]

We previously reported that the first reduction voltage (~2.3 V) of the [DEME][TFSA] electrolytes was slightly lower than those for organic TEGDME electrolytes (~2.5 V). This was explained as the *solvent effect* linked to the solubility of Li_2S_m.[29,30] Because the solubility of Li_2S_m was extremely low in the [DEME][TFSA] and [P13][TFSA] electrolytes, the reduction intermediates, Li_2S_m, can be accommodated as a solid inside the composite cathode. On the other hand, Li_2S_m is more readily stabilized by solvation in the solution, resulting in

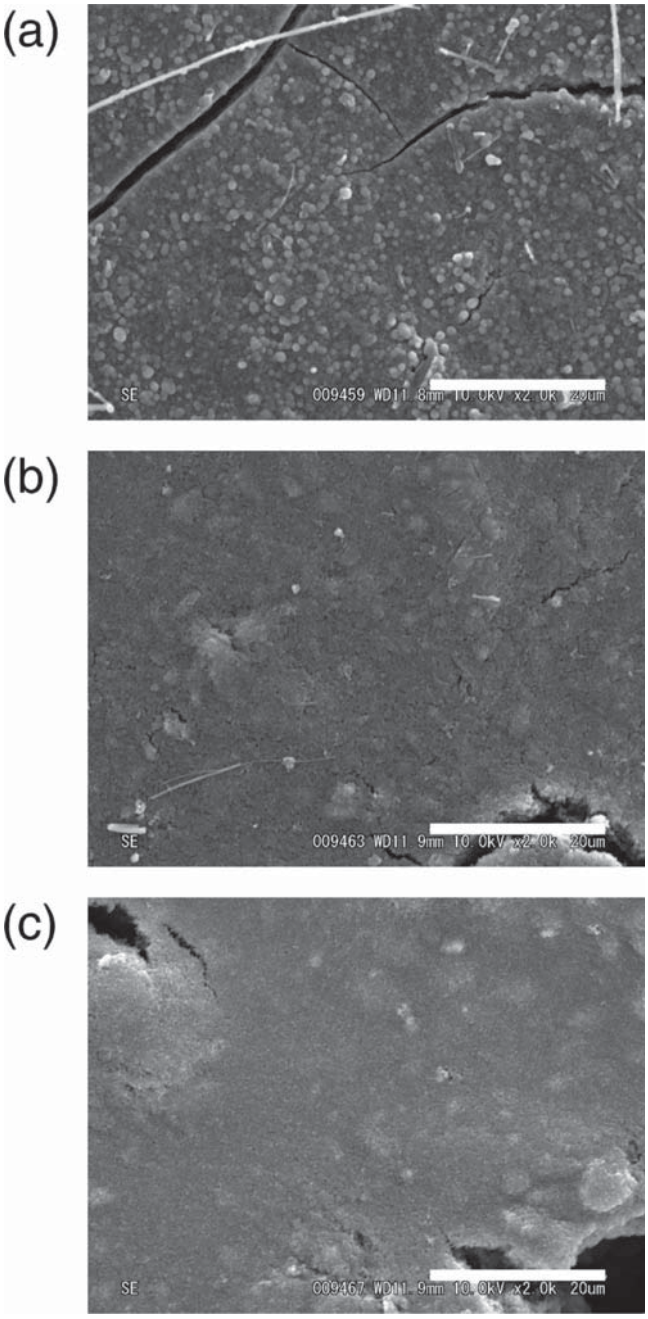

Figure 5. SEM images of KB/S_8 composite cathode surface (a) after 30 charge/discharge cycles in [P13][FSA] electrolyte, (b) after 30 charge/discharge cycles in [P13][TFSA] electrolyte, and (c) in pristine state. Scale bar in each image is 20 μm.

a more positive reduction potential. In the Li−S cell utilizing [P14][OTf], where Li_2S_m is highly soluble, a higher voltage plateau was observed in the discharge curve at ∼2.5 V (Figure 2b). Thus, the same explanation holds for the [P14][OTf] electrolyte as for the TEGDME electrolyte. The uncontrolled dissolution of Li_2S_m in the [P14][OTf] electrolyte also accounts for the poor cycle performance of the Li−S cell (Figure 3): the loss of the active materials from the composite cathode may cause rapid capacity fading, and the redox shuttle can result in a slightly lower efficiency, ∼96%.

The Li−S cell employing [P13][BETA] (Figure 2c) exhibited a high overpotential in the charge/discharge curves, and the initial discharge capacity (∼650 mA·h g^{-1}) was lower than that obtained with the [P13][TFSA] electrolyte (Figure 2a), despite the extremely low solubility of Li_2S_m in both electrolytes. The key difference between these two electrolytes lies in the transport property. As can be seen in Table 1, the [P13][BETA] electrolyte has the highest viscosity of the ILs studied, and its ionic conductivity (σ) and Li^+ diffusion coefficient (D_{Li}) are much lower than those of the other electrolytes. Hence, the poor battery performance in the case of [P13][BETA] is attributed to the higher mass transport resistance in this electrolyte. In fact, the overpotential and initial discharge capacity were greatly improved when the cell was operated at 60 °C (Figure S2). At this temperature, the transport properties of the [P13][BETA] electrolyte (σ = 2.1 mS·cm^{-1} and $D_{Li} = 0.79 \times 10^{-7}$ $cm^2 \cdot s^{-1}$) were comparable to those for the [P13][TFSA] electrolyte at 30 °C.

The charge/discharge performance of the cells employing [DEME]BF_4 and [P13][FSA] electrolytes (Figure 2d and e) was even worse than the case for the [P13][BETA] electrolyte. As shown in Figure 3, the capacity of these batteries decreased drastically within ten charge/discharge cycles in both cases. A similar drastic decay in the capacity of the Li−S cell using [DEME][TFSA] containing $LiBF_4$ as the supporting salt was observed, whereas no obvious failure was observed during the charge/discharge tests when other Li salts such as $LiPF_6$ and Li[BETA] were dissolved in the same IL (Figure S3).

As described earlier for BF_4-based electrolytes, oxidation of polysulfides to sulfur did not occur for evaluating the Li_2S_m solubility in the electrolytes. This implies that the polysulfide species underwent chemical reactions with BF_4^-. ^{11}B and ^{19}F NMR spectra of the polysulfide solution in the electrolytes were measured to validate the occurrence of this possible side reaction. Small peaks were detected around the main peaks of the BF_4 anion in both the ^{11}B and ^{19}F NMR spectra (Figure 4), which suggests the decomposition of the BF_4 anion in the presence of the polysulfides. Moreover, the side reaction is plausibly more pronounced in Li^+-rich solution because a relatively strong peak was found at −152 ppm (^{19}F) for [DEME]BF_4 containing the Li[TFSA] salt (Figure 4a). The nucleophilic attack of polysulfides on the borate center of BF_4^- that interacts with Li^+ plausibly generates byproducts such as LiF and adducts of BF_3 and Li_2S_m. The small NMR peaks may be assigned to the adducts; for example, $[BF_3(LiS_m)]^-$, $[BF_2(LiS_m)_2]^-$, and $[(BF_3)_2(S_m)]^{2-}$ with polysulfides of varying chain lengths.[45] The intrinsically high ionic atmosphere in the IL electrolytes may screen the negative charges of the polysufides and BF_4^-, thus enabling reaction between the anionic species. Similar decomposition of BF_4^- in the presence of Li_2S_m was also observed in a concentrated solution of $LiBF_4$ in the TEGDME electrolyte.[46] Thus, the BF_4 anion may hinder the reversible redox reaction of sulfur/polysulfides in the Li−S cell with IL electrolytes. Zhang et al. reported that $LiPF_6$ also reacts with Li_2S_m in ether-based organic electrolytes.[45] However, we did not observe the apparent side reaction in Li−S cells using 0.5 mol kg^{-1} $LiPF_6$ in [DEME][TFSA] electrolyte (Figure S3). This is probably due to the low solubility of Li_2S_m. The side reaction of Li_2S_m with $LiPF_6$ would become less obvious because Li_2S_m was the least soluble in this electrolyte among [DEME][TFSA] electrolytes containing different Li salts (Figure S1a).

The discharge curves for the [P13][FSA]-based cell shown in Figure 2e are characterized by a plateau voltage of approximately 1.8 V, which is not observed for the other Li−S cells. Moreover, the Coulombic efficiency (discharge

dx.doi.org/10.1021/jp408037e | J. Phys. Chem. C 2013, 117, 20531−20541

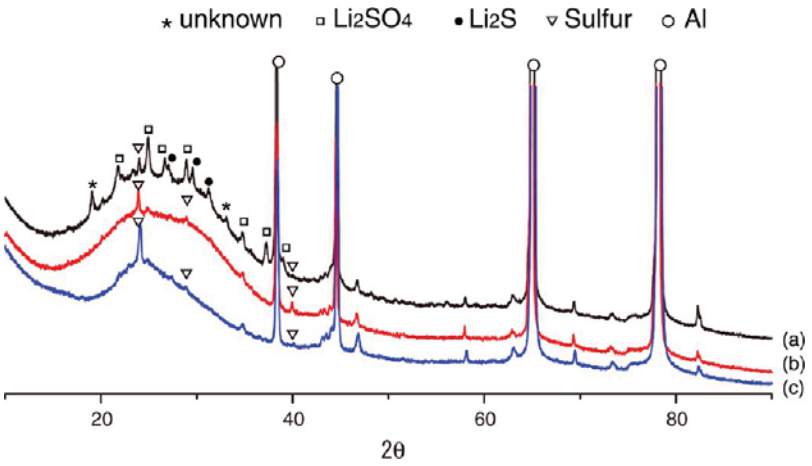

Figure 6. X-ray diffraction patterns of KB/S_8 composite cathode surface corresponding to SEM images is Figure 5 (a) after 30 charge/discharge cycles in [P13][FSA] electrolyte, (b) after 30 charge/discharge cycles in [P13][TFSA] electrolyte, and (c) in pristine state. All the data were acquired in charged state.

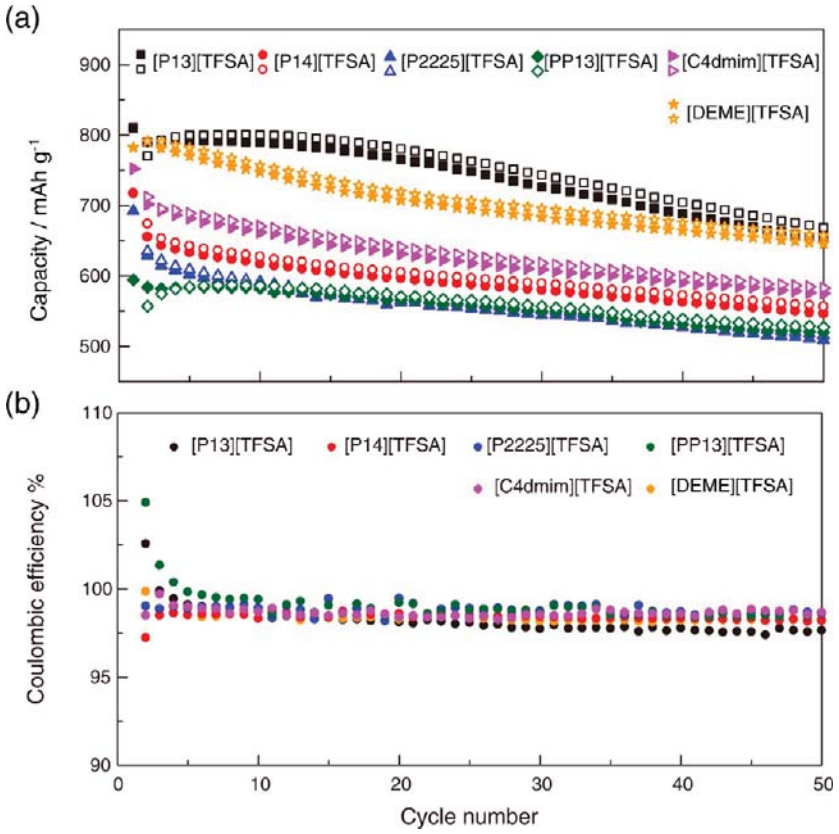

Figure 7. Cycling performance of Li–S cells using [TFSA]-based IL electrolytes with various cations at constant current density of 139 m·Ag^{1-}-sulfur, for (a) capacity, and (b) Coulombic efficiency. Open and closed plots in (a) represent charge and discharge capacities, respectively.

capacity/charge capacity) was higher than 110% (Figure 3). These results strongly support the possibility of an irreversible side reaction during the discharge process. Compared to $[TFSA]^-$ and $[BETA]^-$, $[FSA]^-$ with the $-SO_2F$ group would be less stable in the presence of Li_2S_m. Indeed, the sulfonylfluorides with the $-SO_2F$ group have been used as a precursor for preparing fluorinated sulfonylamide compounds through the reaction with nucleophiles.[47,48] Laruelle et al. reported thermally driven nucleophilic attack of the CH_3O^- group of lithium methoxide on the S–F bond of $[FSA]^-$.[49] Likewise, $[FSA]^-$ may decompose in the presence of nucleophilic polysulfide anions, leading to the disappointing charge/discharge behavior of the Li–S cell. Unlike the BF_4-based electrolytes, there were no detectable differences between the ^1H and ^{19}F NMR spectra of pristine [P13][FSA] and the saturated solution of Li_2S_4 in [P13][FSA]. As shown in Figures 5 and 6, however, the SEM images and XRD spectra conclusively show that solid byproducts were formed on the surface of the KB/S_8 composite cathode after 30 cycles of charge/discharge in the [P13][FSA] electrolyte. Spherical solid particles covering the entire surface of the cathode are observed in the [P13][FSA] electrolyte (Figure 5a); however, they are

dx.doi.org/10.1021/jp408037e | J. Phys. Chem. C 2013, 117, 20531–20541

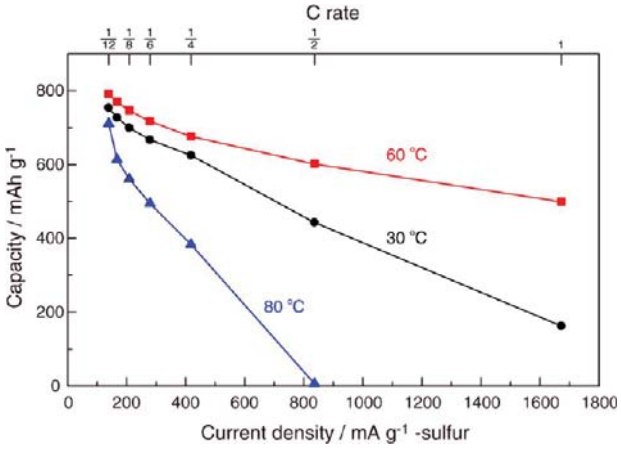

Figure 8. Discharge rate property of Li−S cell using [P13][TFSA] electrolyte containing 0.5 mol·kg^{-1} Li[TFSA] at 30, 60, and 80 °C. Cell was charged at constant current of 139 mA·g^{-1}-sulfur during charging, and discharged at each current density.

not observed in the SEM images of the cathodes in the [P13][TFSA] electrolytes after 30 cycles of charge/discharge (Figure 5b) and before the battery test (Figure 5c). The XRD patterns also show clear differences between the KB/S_8 composite cathode in the [P13][FSA] electrolyte and other electrolytes (Figure 6). The XRD peaks derived from the byproducts that do not appear for the [P13][TFSA] electrolyte and the pristine electrode can be seen in the low-angle region for the [P13][FSA] electrolyte. The peak assignment suggests that the solids may include Li_2SO_4 and Li_2S, though some of the peaks of the byproducts remain unidentified. The surface-insulating layer formed by the decomposition of $[FSA]^-$ is responsible for the drastic increase in the charge-transfer resistance during charge/discharge in this electrolyte (Figure S4). Consequently, [P13][FSA] is not deemed a suitable electrolyte for the Li−S battery, although the dissolution of Li_2S_m is suppressed to a low level in the [P13][FSA] electrolyte (Figure 1) and this electrolyte provides the highest lithium ion conduction among the evaluated IL electrolytes (Table 1).

Figure 7 shows the cycle performance of Li−S cells using [TFSA]-based IL electrolytes with different cationic structures. The difference in the cell performance using the various electrolytes was not very pronounced because of the minimal difference in the solubility of Li_2S_m in these electrolytes, and their solubility values of Li_2S_m were very low (<10 mM in atomic-S concentration, Figure S1b). The charge/discharge curves of all cells were similar to those for [P13][TFSA], i.e., two voltage plateaus (2.3 and 2.0 V) were observed in the discharge curve, and a voltage plateau was observed around 2.4 V in the charge curve (data not shown). The capacity retention of the Li−S cells was approximately 76−87% of the initial discharge capacity after 50 cycles, with high Coulombic efficiency (>98%). The initial capacity ranged from ca. 600 to 800 mA·hg^{-1}, corresponding to 40−50% of the theoretical capacity of sulfur, and increased in the following order based on the cation: $[P13]^+$ > $[DEME]^+$ > $[C_4dmim]^+$ > $[P14]^+$ > $[P2225]^+$ > $[PP13]^+$. This order is in relatively good agreement with the order of the lithium transport properties (σ and D_{Li} in Table 1). This correlation indicates that slower mass transport led to lower utilization of the high capacity of the sulfur cathode, even at a low current density of 139 mA·g^{-1} (1/12 C rate). Thus, the charge/discharge properties of the Li−S cell, such as capacity and rate capability, may be limited by the high viscosity and low lithium ion transport of the IL electrolytes, as is the case for other lithium-ion batteries.[50]

Because the transport properties of IL electrolytes are strongly affected by temperature, the temperature dependence of the Li−S battery performance was also evaluated. Figure 8 shows the discharge rate capability of the Li−S cell employing the [P13][TFSA] electrolyte. By increasing the rate from 139 mA·g^{-1} (1/12 C rate) to 1672 mA·g^{-1} (1 C rate) at 30 °C, the initially high capacity of 750 mA·hg^{-1} was reduced to 160 mA·hg^{-1}. However, the rate capability could be improved by elevating the temperature to 60 °C, where there was an approximately 3-fold increase in σ and D_{Li} compared to their values at 30 °C. Although the capacity gradually decreased with increasing current density, the Li−S cell still afforded a capacity of 500 mA·hg^{-1} even at the current density of 1 C rate at 60 °C. Interestingly, further heating to 80 °C provokes rapid capacity fading of the Li−S cell. This is presumably due to increased dissolution of the active materials at the elevated temperature. This assumption is supported by the observed lower Coulombic efficiency at higher temperature; the Coulombic efficiency was ∼98% at 30 °C and 96% at 60 °C, but was reduced to less than 75% at 80 °C (Figure S5).

4. CONCLUSIONS

The solubility of S_8 and Li_2S_m, and the Li−S cell performance were investigated for a series of aprotic IL-Li salt mixture electrolytes with different cationic and anionic structures. It was demonstrated that the IL solvent is not always effective for suppressing the polysulfide dissolution. It was proposed that the solubility limit of Li_2S_m was governed by the donor ability of the ILs; i.e., the anionic structure of the ILs. Dissolution of Li_2S_m in the strongly basic [P14][OTf] was comparably as high as dissolution in the organic TEGDME electrolyte. In contrast, Li_2S_m dissolution was hampered in the ILs having bulky fluorosulfonyl amide-type anions owing to the weak donor ability of these anions to the Li cation of Li_2S_m. Variation of the cationic structure of [TFSA]-based ILs did not markedly affect the solubility of Li_2S_m. There was also a possible correlation between the ionic size of the ILs and the Li_2S_m solubility: ILs with larger ions exhibited lower solvency for Li_2S_m. Lower Coulombic efficiency and rapid capacity fading were observed for the Li−S battery employing the [P14][OTf] electrolyte because of the presence of highly solubilized Li_2S_m, which led to the unfavorable redox shuttle mechanism and loss of active materials. BF_4^- and $[FSA]^-$ were decomposed in the Li−S cell because of the reaction of these ions with polysulfides, resulting in poor cycle performance. The Li_2S_m dissolution was effectively suppressed in the IL electrolytes containing $[TFSA]^-$, $[BETA]^-$, and PF_6^-; these IL-based electrolytes were electrochemically stable in the Li−S cells although the side reaction between $LiPF_6$ and Li_2S_m was reported in an organic electrolyte.[45] The low Li^+ transport property of ILs at room temperature because of their intrinsically high viscosity has been well recognized as a major shortcoming of IL-based electrolytes. In fact, the viscosity of the ILs prevented rapid charge/discharge of the Li−S cells with high current density at room temperature. However, elevating the temperature to 60 °C allowed the successful operation of the Li−S battery even at 1 C rate because of enhanced Li transport at the higher temperature. However, further heating the battery to 80 °C resulted in the rapid capacity decay and lower Coulombic efficiency, plausibly attributed to the increased solubility of

dx.doi.org/10.1021/jp408037e | J. Phys. Chem. C 2013, 117, 20531−20541

Li_2S_m at higher temperature. Considering the higher viscosity of ILs with [BETA] anions that gives rise to a high overpotential at 30 °C—low-viscosity [TFSA]-based ILs, in particular [P13][TFSA]—were considered optimal for Li−S batteries.

■ ASSOCIATED CONTENT

Supporting Information

The saturation concentrations of S_8 and Li_2S_m in the series of IL-based electrolytes; Charge/discharge curves of Li−S cells at different temperatures and with different Li salts; Nyquist plots of the KB/S_8 composite cathode; battery performance at different temperatures. This material is available free of charge via the Internet at http://pubs.acs.org.

■ AUTHOR INFORMATION

Corresponding Author

*Telephone/Fax: +81-45-339-3955. E-mail: mwatanab@ynu.ac.jp.

Present Address

Jun-Woo Park, Battery Research Group, Korea Electrotechnology Research Institute (KERI), Changwon 641−120, Republic of Korea.

Author Contributions

J.-W. P. and K.U. contributed equally to this work.

Notes

The authors declare no competing financial interest.

■ ACKNOWLEDGMENTS

This study was supported in part by the Advanced Low Carbon Technology Research and Development Program (ALCA) of the Japan Science and Technology Agency (JST) and by the Technology Research Grant Program of the New Energy and Industrial Technology Development Organization (NEDO) of Japan.

■ REFERENCES

(1) Hallett, J. P.; Welton, T. Room-Temperature Ionic Liquids: Solvents for Synthesis and Catalysis. 2. *Chem. Rev.* **2011**, *111*, 3508−3576.

(2) Galinski, M.; Lewandowski, A.; Stepniak, I. Ionic Liquids as Electrolytes. *Electrochim. Acta* **2006**, *51*, 5567−5580.

(3) Lewandowski, A.; Swiderska-Mocek, A. Ionic Liquids as Electrolytes for Li-Ion Batteries-An Overview of Electrochemical Studies. *J. Power Sources* **2009**, *194*, 601−609.

(4) Bruce, P. G.; Freunberger, S. A.; Hardwick, L. J.; Tarascon, J.-M. Li-O_2 and Li-S Batteries with High Energy Storage. *Nat. Mater.* **2012**, *11*, 19−29.

(5) Manthiram, A.; Fu, Y.; Su, Y.-S. Challenges and Prospects of Lithium−Sulfur Batteries. *Acc. Chem. Res.* **2012**, *46*, 1125−1134.

(6) Ji, X.; Nazar, L. F. Advances in Li-S Batteries. *J. Mater. Chem.* **2010**, *20*, 9821−9826.

(7) Ji, X.; Lee, K. T.; Nazar, L. F. A Highly Ordered Nanostructured Carbon-Sulphur Cathode for Lithium-Sulphur Batteries. *Nat. Mater.* **2009**, *8*, 500−506.

(8) Liang, C.; Dudney, N. J.; Howe, J. Y. Hierarchically Structured Sulfur/Carbon Nanocomposite Material for High-Energy Lithium Battery. *Chem. Mater.* **2009**, *21*, 4724−4730.

(9) Jayaprakash, N.; Shen, J.; Moganty, S. S.; Corona, A.; Archer, L. A. Porous Hollow Carbon@Sulfur Composites for High-Power Lithium−Sulfur Batteries. *Angew. Chem., Int. Ed.* **2011**, *50*, 5904−5908.

(10) Zheng, G.; Yang, Y.; Cha, J. J.; Hong, S. S.; Cui, Y. Hollow Carbon Nanofiber-Encapsulated Sulfur Cathodes for High Specific Capacity Rechargeable Lithium Batteries. *Nano Lett.* **2011**, *11*, 4462−4467.

(11) Wang, H.; Yang, Y.; Liang, Y.; Robinson, J. T.; Li, Y.; Jackson, A.; Cui, Y.; Dai, H. Graphene-Wrapped Sulfur Particles as a Rechargeable Lithium−Sulfur Battery Cathode Material with High Capacity and Cycling Stability. *Nano Lett.* **2011**, *11*, 2644−2647.

(12) Zhao, M.-Q.; Liu, X.-F.; Zhang, Q.; Tian, G.-L.; Huang, J.-Q.; Zhu, W.; Wei, F. Graphene/Single-Walled Carbon Nanotube Hybrids: One-Step Catalytic Growth and Applications for High-Rate Li−S Batteries. *ACS Nano* **2012**, *6*, 10759−10769.

(13) Hagen, M.; Dörfler, S.; Althues, H.; Tübke, J.; Hoffmann, M. J.; Kaskel, S.; Pinkwart, K. Lithium−Sulphur Batteries − Binder Free Carbon Nanotubes Electrode Examined with Various Electrolytes. *J. Power Sources* **2012**, *213*, 239−248.

(14) Wu, F.; Chen, J.; Chen, R.; Wu, S.; Li, L.; Chen, S.; Zhao, T. Sulfur/Polythiophene with a Core/Shell Structure: Synthesis and Electrochemical Properties of the Cathode for Rechargeable Lithium Batteries. *J. Phys. Chem. C* **2011**, *115*, 6057−6063.

(15) Gao, J.; Lowe, M. A.; Kiya, Y.; Abruña, H. D. Effects of Liquid Electrolytes on the Charge−Discharge Performance of Rechargeable Lithium/Sulfur Batteries: Electrochemical and in-Situ X-ray Absorption Spectroscopic Studies. *J. Phys. Chem. C* **2011**, *115*, 25132−25137.

(16) Peled, E.; Sternberg, Y.; Gorenshtein, A.; Lavi, Y. Lithium-Sulfur Battery: Evaluation of Dioxolane-Based Electrolytes. *J. Electrochem. Soc.* **1989**, *136*, 1621−1625.

(17) Mikhaylik, Y. V.; Akridge, J. R. Polysulfide Shuttle Study in the Li/S Battery System. *J. Electrochem. Soc.* **2004**, *151*, A1969−A1976.

(18) Shim, J.; Striebel, K. A.; Cairns, E. J. The Lithium/Sulfur Rechargeable Cell: Effects of Electrode Composition and Solvent on Cell Performance. *J. Electrochem. Soc.* **2002**, *149*, A1321−A1325.

(19) Aurbach, D.; Pollak, E.; Elazari, R.; Salitra, G.; Kelley, C. S.; Affinito, J. On the Surface Chemical Aspects of Very High Energy Density, Rechargeable Li−Sulfur Batteries. *J. Electrochem. Soc.* **2009**, *156*, A694−A702.

(20) Zhang, S. S.; Read, J. A. A New Direction for the Performance Improvement of Rechargeable Lithium/Sulfur Batteries. *J. Power Sources* **2012**, *200*, 77−82.

(21) Lin, Z.; Liu, Z.; Fu, W.; Dudney, N. J.; Liang, C. Phosphorous Pentasulfide as a Novel Additive for High-Performance Lithium-Sulfur Batteries. *Adv. Funct. Mater.* **2013**, *23*, 1064−1069.

(22) Ji, X.; Evers, S.; Black, R.; Nazar, L. F. Stabilizing Lithium−Sulphur Cathodes Using Polysulphide Reservoirs. *Nat. Commun.* **2011**, *2*, 325.

(23) Jeong, S. S.; Lim, Y. T.; Choi, Y. J.; Cho, G. B.; Kim, K. W.; Ahn, H. J.; Cho, K. K. Electrochemical Properties of Lithium Sulfur Cells Using PEO Polymer Electrolytes Prepared Under Three Different Mixing Conditions. *J. Power Sources* **2007**, *174*, 745−750.

(24) Hayashi, A.; Ohtomo, T.; Mizuno, F.; Tadanaga, K.; Tatsumisago, M. All-Solid-State Li/S Batteries with Highly Conductive Glass−Ceramic Electrolytes. *Electrochem. Commun.* **2003**, *5*, 701−705.

(25) Kobayashi, T.; Imade, Y.; Shishihara, D.; Homma, K.; Nagao, M.; Watanabe, R.; Yokoi, T.; Yamada, A.; Kanno, R.; Tatsumi, T. All Solid-State Battery with Sulfur Electrode and Thio-LISICON Electrolyte. *J. Power Sources* **2008**, *182*, 621−625.

(26) Zhang, S. S. New Insight into Liquid Electrolyte of Rechargeable Lithium/Sulfur Battery. *Electrochim. Acta* **2013**, *97*, 226−230.

(27) Yuan, L. X.; Feng, J. K.; Ai, X. P.; Cao, Y. L.; Chen, S. L.; Yang, H. X. Improved Dischargeability and Reversibility of Sulfur Cathode in a Novel Ionic Liquid Electrolyte. *Electrochem. Commun.* **2006**, *8*, 610−614.

(28) Tachikawa, N.; Yamauchi, K.; Takashima, E.; Park, J.-W.; Dokko, K.; Watanabe, M. Reversibility of Electrochemical Reactions of Sulfur Supported on Inverse Opal Carbon in Glyme-Li Salt Molten Complex Electrolytes. *Chem. Commun.* **2011**, *47*, 8157−8159.

(29) Park, J.-W.; Yamauchi, K.; Takashima, E.; Tachikawa, N.; Ueno, K.; Dokko, K.; Watanabe, M. Solvent Effect of Room Temperature Ionic Liquids on Electrochemical Reactions in Lithium−Sulfur Batteries. *J. Phys. Chem. C* **2013**, *117*, 4431−4440.

(30) Dokko, K.; Tachikawa, N.; Yamauchi, K.; Tsuchiya, M.; Yamazaki, A.; Takashima, E.; Park, J.-W.; Ueno, K.; Seki, S.; Serizawa,

N.; Watanabe, M. Solvate Ionic Liquid Electrolyte for Li−S Batteries. *J. Electrochem. Soc.* **2013**, *160*, A1304−A1310.
(31) Freemantle, M. Designer Solvents. *Chemical & Engineering News Archive* **1998**, *76*, 32−37.
(32) Tokuda, H.; Hayamizu, K.; Ishii, K.; Abu Bin Hasan Susan, M.; Watanabe, M. Physicochemical Properties and Structures of Room Temperature Ionic Liquids. 1. Variation of Anionic Species. *J. Phys. Chem. B* **2004**, *108*, 16593−16600.
(33) Muldoon, M. J.; Gordon, C. M.; Dunkin, I. R. Investigations of Solvent-Solute Interactions in Room Temperature Ionic Liquids Using Solvatochromic Dyes. *J. Chem. Soc., Perkin Trans. 2* **2001**, 433−435.
(34) Tokuda, H.; Tsuzuki, S.; Susan, M. A. B. H.; Hayamizu, K.; Watanabe, M. How Ionic Are Room-Temperature Ionic Liquids? An Indicator of the Physicochemical Properties. *J. Phys. Chem. B* **2006**, *110*, 19593−19600.
(35) Noda, A.; Hayamizu, K.; Watanabe, M. Pulsed-Gradient Spin-Echo ^{1}H and ^{19}F NMR Ionic Diffusion Coefficient, Viscosity, and Ionic Conductivity of Non-Chloroaluminate Room-Temperature Ionic Liquids. *J. Phys. Chem. B* **2001**, *105*, 4603−4610.
(36) Hayamizu, K.; Aihara, Y.; Nakagawa, H.; Nukuda, T.; Price, W. S. Ionic Conduction and Ion Diffusion in Binary Room-Temperature Ionic Liquids Composed of $EmimBF_4$ and $LiBF_4$. *J. Phys. Chem. B* **2004**, *108*, 19527−19532.
(37) Brouillette, D.; Perron, G.; Desnoyers, J. E. Apparent Molar Volume, Heat Capacity, and Conductance of Lithium Bis-(trifluoromethylsulfone)imide in Glymes and Other Aprotic Solvents. *J. Solution Chem.* **1998**, *27*, 151−182.
(38) Umebayashi, Y.; Mitsugi, T.; Fukuda, S.; Fujimori, T.; Fujii, K.; Kanzaki, R.; Takeuchi, M.; Ishiguro, S. I. Lithium Ion Solvation in Room-Temperature Ionic Liquids Involving Bis-(trifluoromethanesulfonyl)imide Anion Studied by Raman Spectroscopy and DFT Calculations. *J. Phys. Chem. B* **2007**, *111*, 13028−13032.
(39) Tobishima, S. I.; Yamamoto, H.; Matsuda, M. Study on the Reduction Species of Sulfur by Alkali Metals in Nonaqueous Solvents. *Electrochim. Acta* **1997**, *42*, 1019−1029.
(40) Schmeisser, M.; Illner, P.; Puchta, R.; Zahl, A.; van Eldik, R. Gutmann Donor and Acceptor Numbers for Ionic Liquids. *Chem.—Eur. J.* **2012**, *18*, 10969−10982.
(41) Hayamizu, K.; Tsuzuki, S.; Seki, S.; Fujii, K.; Suenaga, M.; Umebayashi, Y. Studies on the Translational and Rotational Motions of Ionic Liquids Composed of N-methyl-N-propyl-pyrrolidinium (P-13) Cation and Bis(trifluoromethanesulfonyl)amide and Bis-(fluorosulfonyl)amide Anions and Their Binary Systems Including Lithium Salts. *J. Chem. Phys.* **2010**, 133.
(42) Fujii, K.; Hamano, H.; Doi, H.; Song, X.; Tsuzuki, S.; Hayamizu, K.; Seki, S.; Kameda, Y.; Dokko, K.; Watanabe, M.; Umebayashi, Y. Unusual Li^+ Ion Solvation Structure in Bis(fluorosulfonyl)amide Based Ionic Liquid. *J. Phys. Chem. B* [Online early access] DOI: 10.1021/jp4053264. Published Online: September 13, 2013.
(43) Kobrak, M. N. The Relationship Between Solvent Polarity and Molar Volume in Room-Temperature Ionic Liquids. *Green Chem.* **2008**, *10*, 80−86.
(44) Lui, M. Y.; Crowhurst, L.; Hallett, J. P.; Hunt, P. A.; Niedermeyer, H.; Welton, T. Salts Dissolved in Salts: Ionic Liquid Mixtures. *Chem. Sci.* **2011**, *2*, 1491−1496.
(45) Zhang, S. S. Liquid Electrolyte Lithium/Sulfur Battery: Fundamental Chemistry, Problems, and Solutions. *J. Power Sources* **2013**, *231*, 153−162.
(46) Ueno, K.; Park, J.-W.; Yamazaki, A.; Mandai, T.; Tachikawa, N.; Dokko, K.; WatanabeM.Anionic Effects on Solvate Ionic Liquid Electrolytes in Rechargeable Lithium-Sulfur Batteries. *J. Phys. Chem. C* [Online early access] DOI: 10.1021/jp407158y. Published Online: September 16, 2013.
(47) Toulgoat, F.; Langlois, B. R.; Médebielle, M.; Sanchez, J.-Y. Efficient Preparation of New Fluorinated Lithium and Ammonium Sulfonimides. *J. Org. Chem.* **2008**, *73*, 5613−5616.
(48) Hallac, B. B.; Geiculescu, O. E.; Rajagopal, R. V.; Creager, S. E.; DesMarteau, D. D. Lithium-Conducting Ionic Melt Electrolytes from Polyether-Functionalized Fluorosulfonimide Anions. *Electrochim. Acta* **2008**, *53*, 5985−5991.
(49) Eshetu, G. G.; Grugeon, S.; Gachot, G.; Mathiron, D.; Armand, M.; Laruelle, S. LiFSI vs. $LiPF_6$ Electrolytes in Contact with Lithiated Graphite: Comparing Thermal Stabilities and Identification of Specific SEI-Reinforcing Additives. *Electrochim. Acta* **2013**, *102*, 133−141.
(50) Park, J.-W.; Yoshida, K.; Tachikawa, N.; Dokko, K.; Watanabe, M. Limiting Current Density in Bis(trifluoromethylsulfonyl)amide-Based Ionic Liquid for Lithium Batteries. *J. Power Sources* **2011**, *196*, 2264−2268.